

Parametric Finite Element Analysis of Belt Type Assembly of PEMFC

Guoqing LIU^a, Zhendong ZHAO^a, Jinguo WU^{a,1} and Wei HUANG^b

^a*School of Automotive & Rail Transit, Nanjing Institute of Technology, Nanjing 211167, China*

^b*Jiangsu Yao Yang New Energy Technology Co. LTD, Yangzhou 225006, China*

Abstract. The belt type assembly of proton exchange membrane fuel cell is more compact and have higher power density than the screw assembly method. The uniform distribution of fuel cell stack clamping load directly affects the efficiency, reliability and durability of the stack. The design of high-strength and light-weight packaging structure is conducive to improving the lightweight level of the whole stack system. In this paper, the finite element model of the belt type clamping stack was established by numerical simulation, and the effects of the number of belts and endplate radius on the stress of the stack and the clamping structure were analyzed. The results reveal that increasing the number of belts can improve the uniformity of contact pressure distribution inside the stack, increasing the width of the belt can improve the bearing capacity of the belt and the uniformity of the contact pressure of the stack better than increasing its thickness. When different numbers of belts are clamping, the stress of each belt is not consistent, and the middle belt first yields. Increasing the endplate radius has little effect on the uniformity of the contact pressure distribution of the stack, but can improve the bearing capacity of the belt.

Keywords. Belt, proton exchange membrane fuel cell, lightweight, uniformity of contact pressure

1. Introduction

Proton exchange membrane fuel cell (PEMFC) has become one of the most studied and widely used fuel cells because of its small size, high power density and high energy conversion efficiency [1-3]. PEMFC is mainly composed of endplates, insulating plates, collector plates, bipolar plates and membrane electrodes assembly [4]. As the PEMFC single cell is only 0.7V~1.2V under rated operating conditions, the performance is far from adequate to meet the actual demand. In practical applications, hundreds of single cells are usually stacked, and the stack with different output power is designed by means of series stacking or by varying the area of membrane electrode assembly (MEA). After the stack has been connected in series, the stack must also be clamped through a reasonable clamping load [5-6]. The distribution of clamping load has a great influence on the uniformity of contact pressure inside the stack. Uneven distribution of contact

¹ Corresponding author, Jinguo Wu, School of Automotive & Rail Transit, Nanjing Institute of Technology, Nanjing 211167, China; E-mail: wujg8848@163.com.

This work received the financial supports from the 16th batch of 'six talent peaks' Foundation of Jiangsu Province, China (Grants No. 2019-JXQC-005) and the Natural Science Foundation of Jiangsu Province, China (Grants No. BK20191009).

pressure can cause uneven distribution of current density, resulting in local hot spots and other phenomena, leading to serious corrosion in some areas of the stack and reducing the durability of fuel cell [7-8].

In order to improve the contact pressure uniformity, many scholars have conducted detailed studies on the pressure distribution in the stack. Hou Yongping [9] analyzed and concluded that the magnitude of MEA contact pressure for each level of single cell within a 10-layer stack was essentially the same, but the contact pressure uniformity within a single MEA varied by up to 30.87%. Alizadeh [10] study the contact pressure of single, 3 and 15 cells, and the results showed that the contact pressure of GDL increased with the number of cells, and the contact pressure of the intermediate cells was more uniformly distributed compared to the external cells near the endplate. Chun tientung [11] et al. pointed out that the variation and uneven pressure distribution of the fuel cell stack are mainly caused by the unsuitable mechanical response of the stacked cell-units and the clamping method, and proposed design guidelines for the stack improvement. Ding Yi [12] et al. studied the influence of the number and distribution of belts and the endplate radius on the MEA contact pressure, and the results showed that the number and distribution of belts had a significant influence on the magnitude of the contact pressure between MEA and metal pole plate and its uniformity, and the uniformity of MEA contact pressure was better for 4 and 5 belts; the uniformity of MEA contact pressure slightly decreased when the radius of endplate increased. The uneven pressure distribution inside the stack is mainly due to the deformation of the endplate [3]. To avoid this phenomenon, a common method is to increase the thickness of the endplate [13]. Zhang Zhiming [14] pointed out that the thickness of the endplate can be reduced by using a larger number of belts. Liu Bo [15] et al. optimized the endplate topology design for the belts clamping structure to reduce the endplate weight while improving the uniformity of contact pressure distribution.

Belt type packaging structure has been used in recent years due to its unique advantages. Based on the equivalent stiffness model, this paper studies the effects of the number, width, thickness of belts and the endplate radius on the stress distribution between the inside of the stack and the belts by using the COMSOL Musipysics.

2. Finite Element Modeling and Evaluation Metric of Stack Assembled by Belts

2.1. Material Parameters

In this paper, the equivalent stiffness model of the fuel cell stack is established based on the experimentally obtained load-displacement data, and the load-displacement curve of the stack is shown in Fig. 1 The equivalent stiffness is converted into the material mechanics model parameters of the stack by equivalent stiffness calculation.

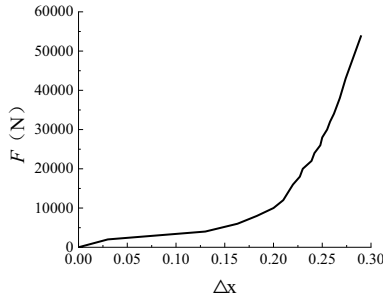


Figure 1. Load-displacement curve.

In addition, finite element models including belts, endplate, insulation board and copper electrode were also developed. The material parameters of each component in the model are shown in Table 1.

Table 1. Material parameters.

Material	Density (kg/m ³)	Young's modulus (MPa)	Poisson's ratio	Yield strength (MPa)
endplate	2.78×10^3	71×10^3	0.33	260
insulation board	1.96×10^3	76×10^3	0.25	690
copper electrode	8.94×10^3	115×10^3	0.34	310
steel belt	7.98×10^3	195×10^3	0.3	281

For materials such as endplate and insulation board, they are viewed as linear elastic materials because they are not allowed to enter the yielding stage or are not concerned with their specific force conditions; for belts, they are set as ideal plastic materials because they need to analyze their mechanical change behavior after entering the plastic yielding state, but are not concerned with their mechanical hardening behavior after entering the yielding state.

2.2. Boundary Conditions

The finite element model established in this paper is 1/2 symmetric model, so symmetric boundary conditions are imposed on the symmetric surface. The assembly relationship between the components of the PEMFC stack is contact relationship, and the friction coefficient of each contact relationship is 0.1. In order to analyze the influence of the belts on the uniformity of the contact pressure inside the stack and the force distribution of the belts, the clamping force is kept consistent in different simulation cases. The specified displacement of the belts is set to 15 mm, and the 3D finite element model of PEMFC is shown in Fig. 2.

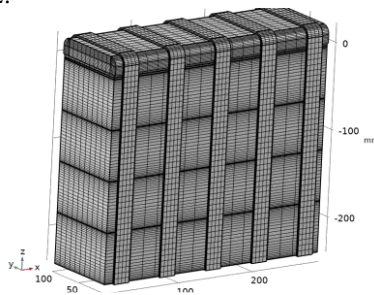


Figure 2. Finite element model of PEMFC.

2.3. Evaluation Metric

Under the action of clamping load, the contact pressure of the outer stack is more unevenly distributed than the inner one, so this paper analyzes the contact pressure uniformity on the outermost first stack surface. For quantitative comparison, the coefficient of variation (CV) is used as the evaluation index of contact pressure uniformity [9], and the coefficient of variation α is defined as:

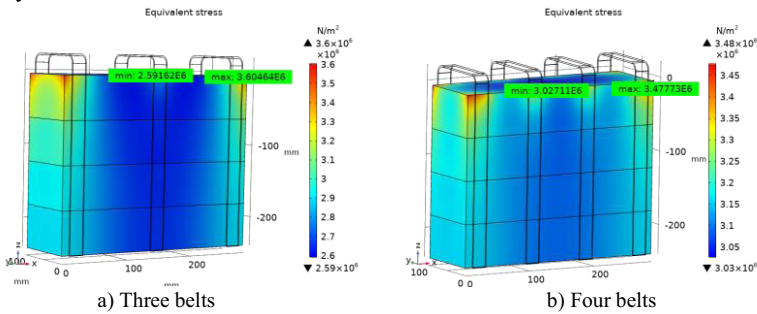
$$\alpha = \frac{R}{\mu} = \frac{\sqrt{\int_0^L (\sigma - \mu)^2 dx^2}}{L^2} \bigg/ \frac{1}{L} \int_0^L p dx \tag{1}$$

where μ is the mean value, R is the standard deviation, and L is the integration path length. The smaller the value of α , the more uniform the stress distribution.

3. Results and Discussion

3.1. Stress Analysis of the Stack Under Different Belt Arrangement Schemes

The stack is clamped by endplates and belts. The structure and dimensions of the endplates and belts, as well as the number of belts and the form of their distribution can have a significant influence on the stress and deformation of the stack. Therefore, it is necessary to analyze the stress and deformation of the stack with different number of belts arrangements. Fig. 3 shows the stress distribution of the stack with 2mm thickness, 20mm width and 3-6 belts. It can be clearly seen that the stress value of the stack near the endplate is higher, and the stress amplitude appears in the stack at the location where the belts appear. With the increase of the number of belts, the maximum stress value of the stack tends to decrease, the minimum stress tends to increase, and the overall stress uniformity of the stack tends to be better.



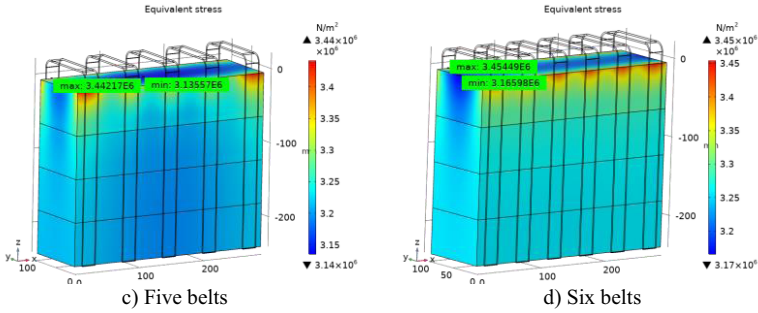


Figure 3. Stress distribution in the stack when the belt width is constant and the number of belts is increased.

For quantitative comparison, the surface of the stack near the endplate is selected for clamping structures with different number and width of belts, and its equivalent stress distribution is statistically shown in Table 2. It can be seen that when the belt width is constant and the number of belts is increased, the value of the CV decreases, and the stress distribution on the surface of the stack is more uniform. With the same number of belts, the CV decreases with the increase of belt width. When the total weight of belts is limited and the number of belts is changed, the value of CV also decreases with the increase of the number of belts. In summary, increasing the number and width of belts can make the equivalent stress distribution of the stack more uniform. From the perspective of light weight, the number of belts should be increased as much as possible when the total weight of belts is limited.

Table 2. Statistics of the equivalent stress distribution on the surface of the stack near the endplate.

Number of belts	Belt width (mm)	Total mass of belt (kg)	Mean value(N/m ²)	Standard deviation(N/m ²)	CV (α)	Maximum (N/m ²)
1	289.5	5.3855	3.434E+06	6.809E+04	0.0198	3.581E+06
	20	0.7441	2.229E+06	5.765E+05	0.2587	3.823E+06
2	25	0.9302	2.500E+06	6.456E+05	0.2582	4.269E+06
	75	2.7905	3.158E+06	1.448E+05	0.0459	3.470E+06
3	20	1.1162	2.819E+06	2.616E+05	0.0928	3.605E+06
	25	1.3952	2.977E+06	1.747E+05	0.0587	3.515E+06
4	50	2.7905	3.193E+06	7.493E+04	0.0235	3.386E+06
	20	1.4883	3.148E+06	1.019E+05	0.0324	3.478E+06
5	25	1.8603	3.219E+06	8.918E+04	0.0277	3.486E+06
	37.5	2.7905	3.320E+06	7.516E+04	0.0226	3.572E+06
6	20	1.8603	3.222E+06	7.747E+04	0.0241	3.442E+06
	25	2.3254	3.280E+06	7.461E+04	0.0228	3.476E+06
6	30	2.7905	3.320E+06	7.547E+04	0.0227	3.503E+06
	20	2.2323	3.270E+06	7.580E+04	0.0232	3.454E+06
6	25	2.7905	3.319E+06	7.772E+04	0.0234	3.494E+06

The cloud diagram of contact pressure distribution on the surface of the stack near the endplate is shown in Figure 4. It can be more obviously seen that the contact pressure distribution at the edge of the stack is highly correlated with the number of belts and the distribution position, and increasing the number of belts will make the contact pressure distribution more uniform.

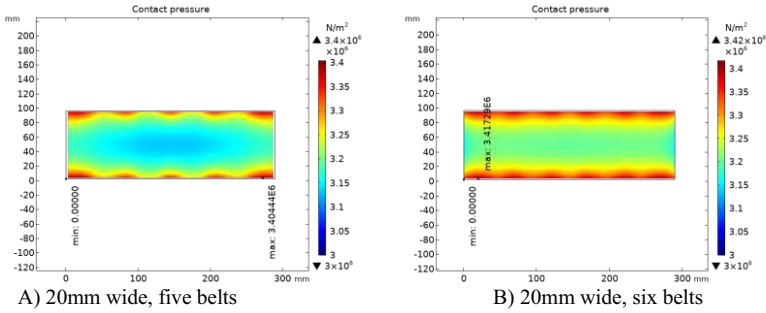


Figure 4. Cloud map of contact pressure distribution on the surface of the stack near the endplate.

Under different number and width belt clamps, the stack surface near the endplate selects a section along the length direction (X direction) and width direction (Y direction), and its equivalent stress distribution is shown in Figure 5 (a) and Figure 5 (b) respectively. It can be seen that along the length direction, the stress value is higher at the position where the belt appears, while the stress value is lower in the middle of the two belts. Increasing the number of belts can obviously make the stress on the stack near the endplate more uniform. Along the width direction, because the section line is selected in the middle, when the number of belts is odd, the stress values on both sides of the stack are high and the middle is low; When the number of belts is even, the stress value in the middle of the stack is higher, and the stress value on both sides is lower.

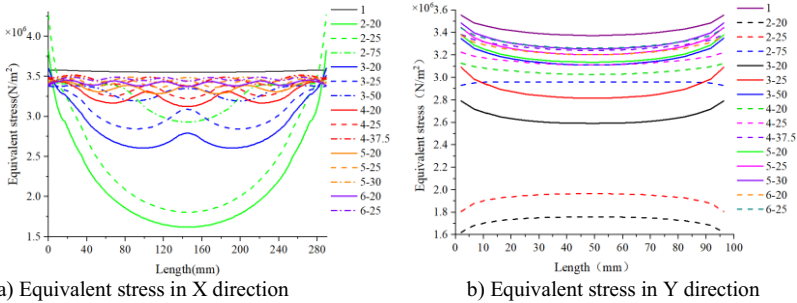


Figure 5. Equivalent stress distribution along the length direction of the stack near the endplate.

3.2. Analysis on the Stress Strength of Belt Under Different Belt Arrangement Schemes

Fig. 6 shows the stress distribution of the belts when the width of the belts is 20 mm and the number of belts is 5 and 6 respectively, and the thickness of the belts is 2 mm. It can be seen that the stress value in the horizontal section (y-direction) where the belts are in contact with the endplate is significantly smaller, and the stress value in the vertical section (z-direction) of the belts is larger.

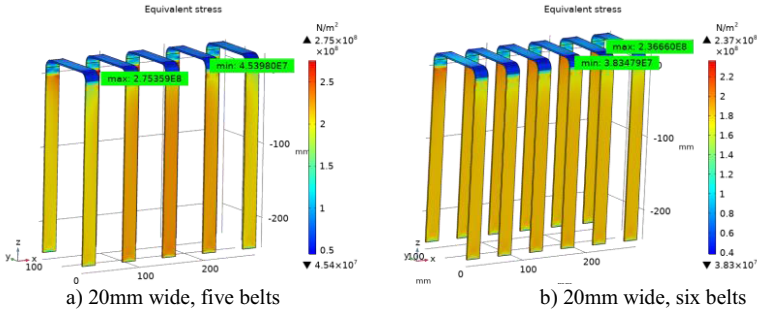


Figure 6. Stress distribution of the belts when the belt width is constant and the number of belts is increased.

The statistics of the force distribution of each belt for different number of belts and belts width are shown in Table 3. Because of the symmetry of the structure, only half of the number of belts were selected for the statistics. Obviously, as the number of belts increases, the maximum and minimum stresses on the belts show a decreasing trend, which is due to the fact that the applied clamped load is constant at the same compression amount, and increasing the number of belts can reduce the stress on a single belt. When the number of belts is the same, increasing the width of the belts can reduce the maximum stress on the belts. And when the total weight of the belts is limited, decreasing the width of the belts and increasing the number of belts can reduce the maximum stress on the belts.

Table 3. Stress distribution statistics of the belt.

Number of belts	Belt width (mm)	Number of belts (kg)	Left 1 belt		Left 2 belt		Left 3 belt			
			Maximum (N/m ²)	Minimum (N/m ²)	Maximum (N/m ²)	Minimum (N/m ²)	Maximum (N/m ²)	Minimum (N/m ²)		
1	289.5	5.3855	1.44E+08	1.92E+07						
	20	0.7441	2.81E+08	7.18E+07						
2	25	0.9302	2.81E+08	5.56E+07						
	75	2.7905	2.81E+08	2.23E+07						
	20	1.1162	2.81E+08	6.12E+07					2.81E+08	4.88E+07
3	25	1.3952	2.81E+08	5.23E+07	2.81E+08	6.23E+07				
	50	2.7905	2.34E+08	3.62E+07	2.23E+08	4.11E+07				
4	20	1.4883	2.81E+08	5.21E+07	2.81E+08	5.47E+07				
	25	1.8603	2.76E+08	4.79E+07	2.81E+08	5.03E+07				
	37.5	2.7905	1.95E+08	4.07E+07	1.99E+08	4.01E+07				
5	20	1.8603	2.65E+08	4.63E+07	2.75E+08	4.55E+07	2.73E+08	4.62E+07		
	25	2.3254	2.30E+08	4.34E+07	2.24E+08	4.12E+07	2.24E+08	4.09E+07		
	30	2.7905	1.89E+08	4.13E+07	1.86E+08	3.64E+07	1.83E+08	3.55E+07		
6	20	2.2323	2.29E+08	4.25E+07	2.28E+08	3.96E+07	2.29E+08	3.82E+07		
	25	2.7905	2.01E+08	3.91E+07	1.83E+08	3.48E+07	1.79E+08	3.27E+07		

When four or less belts are used, the maximum stress on the belt has reached 281MPa, which is the yield strength of the material. Due to the ideal plasticity of the material intrinsic structure setting, the stress no longer grows after reaching the yield strength, although the deformation increases.

3.3. Stress Analysis Under Different Endplate Radius

The change of the endplate radius will change the deformation state of the belts after tensioning, thus affecting the stress distribution of the stack, the belts and the stress of

the endplate. In order to analyze the internal stress of the stack with different endplate radius, the stress distribution of the stack, belts and endplate are shown in Tables 4 and Table 5 when the radius are 1/4, 2/4, 3/4 and 1 of the thickness of the endplate under five 20mm width belts.

It can be seen from table 4 that the influence of the change of the endplate radius on the uniformity of the contact pressure distribution of the stack is almost negligible. However, a larger radius can effectively reduce the quality of the endplate. Therefore, the large endplate radius can be selected to realize the overall structure lightweight.

Table 4. Statistics of contact pressure distribution on the surface of the stack near the endplate.

Endplate radius (mm)	Total mass of endplate (kg)	Mean value (N/m ²)	Standard deviation (N/m ²)	CV (α)	Mean value (N/m ²)
5	1.5736	3.032E+06	7.099E+05	0.2342	3.400E+06
10	1.5477	3.033E+06	7.102E+05	0.2342	3.404E+06
15	1.5045	3.031E+06	7.098E+05	0.2342	3.400E+06
20	1.4441	3.029E+06	7.095E+05	0.2342	3.417E+06

Table 5 shows the maximum stress statistics of endplates and belts. It can be concluded that under the same thickness of endplates, increasing the radius of endplates can effectively reduce the maximum stress value of endplates, but at the same time, the maximum stress value of belts has also increased.

Table 5. Maximum stress statistics for endplates and belts.

Endplate radius (mm)	Maximum endplate stress (N/m ²)	Maximum belt stress (N/m ²)
5	1.159E+08	2.652E+08
10	1.288E+08	2.754E+08
15	9.108E+07	2.745E+08
20	8.636E+07	2.810E+08

3.4. Optimization of Belt Thickness and Size

Based on lightweight consideration, parametric modeling and simulation of the width and thickness of the belts are carried out for the clamping structure of five belts, in order to optimize the dimensions of the belts (such as width and thickness) and realize the lightweight of the clamping structure of the belts while meeting the strength requirements.

The size series of belts selected for the simulation are shown in Table 6. There are three sizes of belts: 15 mm, 17.5 mm, and 20 mm in width, and four thickness sizes under each width, for a total of 12 combinations. According to the previous analysis, although the five belts have the same length and size, the stress distribution on each belt is different, and the five belts do not reach the yield state at the same time, but in sequence. For this reason, only three belts were selected for analysis according to the symmetry, and the compression of the stack when each belt reached the permissible stress was calculated as shown in Table 6. As the thickness of the belts increases, the compression of the stack that each belt can carry when it reaches the permissible stress also increases gradually. It can be seen that increasing the width of the belts is more beneficial than increasing the thickness to improve the loading strength of the belts under the similar mass.

Table 6. Simulation of the selected belt size series.

Serial number	Width /mm	Thickness /mm	Total mass of belt /kg	Compression of the stack when the belt reaches the permissible stress /mm		
				Belt 1	Belt 2	Belt 3
01	15	1.5	1.0449	12.9	12.75	12.75
02		2.0	1.3952	13.8	13.5	13.5
03		2.5	1.7463	14.1	13.8	13.8
04	17.5	3.0	2.0984	14.55	14.25	14.25
05		1.25	1.0152	12.9	12.75	12.9
06		1.75	1.4234	13.8	13.65	13.5
07	20	2.25	1.8325	14.4	13.95	14.25
08		2.75	2.2427	14.7	14.55	14.55
09		1.0	0.9276	12.9	12.6	12.75
10	20	1.5	1.3932	13.65	13.65	13.5
11		2.0	1.8603	14.55	14.25	14.25
12		2.5	2.3286	14.85	14.7	14.7

4. Conclusions

The pressure homogeneity of the fuel cell stack has an important impact on its performance. The design of high-strength and lightweight clamping structure is beneficial to enhance the light weight of the whole stack system. In this paper, we studied and analyzed the force characteristics and laws of the belt-clamped stack under different assembly schemes by numerical simulation methods, and draw the following conclusions:

- 1) The contact pressure distribution of the stack near the endplate is highly correlated with the number of belts and the distribution position. Increasing the number and width of belts to load the assembly load more uniformly on the stack can improve the stress uniformity of the stack near the endplate.
- 2) When the total weight of the belts is limited, decreasing the width of the belts and increasing the number of belts can reduce the maximum stress on the belts when the thickness of the belts is certain. When the number of belts is certain, increasing the width of the belts is better than increasing their thickness to improve the load-bearing capacity of the belts. When different numbers of belts are clamped, the stresses of each belt are not uniform, and generally the middle belt is subjected to greater stresses and is the first to yield.
- 3) Appropriate increase in the size of the radius of the endplate transition corners can reduce the stress concentration at the corners of the belts and improve the load-bearing capacity of the belts.

References

- [1] Weng LF, Jhuang JW, Bhavanari M, et, al. Effects of assembling method and force on the performance of proton-exchange membrane fuel cells with metal foam flow field. *International Journal of Energy Research*. 2020 Dec; 44(12):9707-9713.
- [2] Barzegari MM, Ghadimi M, Momenifar M, et, al. Investigation of contact pressure distribution on gas diffusion layer of fuel cell with pneumatic endplate. *Applied Energy*. 2020 Feb; 263:114663-114663.
- [3] Mostafa H, Mohammadreza S, Peyman GT, et, al. Optimization of proton exchange membrane fuel cell's end plates. *SN Applied Sciences*. 2020 Jul; 2(8):1-10.
- [4] Qiu DK, Yi PY, Peng LF, et, al. Assembly design of proton exchange membrane fuel cell stack with stamped metallic bipolar plates. *International Journal of Hydrogen Energy*. 2015 Mar; 40(35):11559-11568.

- [5] Zhou ZH, Qiu DK, Zhai S, et al. Investigation of the assembly for high-power proton exchange membrane fuel cell stacks through an efficient equivalent model. *Applied Energy*. 2020 Jul; 277.
- [6] Liu LF, Liu B, Wu CW, et, al. Reliability prediction of large fuel cell stack based on structure stress analysis. *Journal of Power Sources*. 2017 Jun; 363:95-102.
- [7] Peng LF, Shao H, Qiu DK, et, al. Investigation of the non-uniform distribution of current density in commercial-size proton exchange membrane fuel cells. *Journal of Power Sources*. 2020 Feb; 453(C):227836-227836.
- [8] Lilavivat V, Shimpalee S, Van Zee JW, et, al. Current Distribution Mapping for PEMFCs. *Electrochimica Acta*. 2015 Jun; 174:1253-1260.
- [9] Hou YP, Lin L, Ma LY, et, al. Effect of Clamping load on the performance and contact pressure of PEMFC stack // WCX World Congress Experience. 2018.
- [10] Alizadeh E, Barzegari MM, Momenifar M, et, al. Investigation of contact pressure distribution over the active area of PEM fuel cell stack. *International Journal of Hydrogen Energy*. 2016 Dec; 41(4): 3062-3071.
- [11] Chung TT, Lin CT, Shiu HR, et al. Mechanical design and analysis of a proton exchange membrane fuel cell stack. *Journal of the Chinese Institute of Engineers*. 2016 Apr; 39(3):353-362.
- [12] Ding Y, Liang P, Peng LF. Simulation of belt type assembly of PEMFC. *Machine Design and Research*. 2018 Dec; 34(06): 147-151.
- [13] Asghari S, Shahsamandi MH, Ashraf Khorasani MR. Design and manufacturing of end plates of a 5kW PEM fuel cell. *International Journal of Hydrogen Energy*. 2010 Feb; 35(17): 9291-9297.
- [14] Zhang ZM, Shang YP, Tong Z. An equivalent mechanical model investigating endplates deflection for PEM fuel cell stack. *Advances in Mechanical Engineering*. 2021 Jun; 13(7): 1-14.
- [15] Liu B, Wei MY, Ma GJ, et, al. Stepwise optimization of endplate of fuel cell stack assembled by steel belts. *International Journal of Hydrogen Energy*. 2016 Dec; 41(4): 2911-2918.